

Surface electron mobility over a helium film

Déborá Coimbra,¹ Sviatoslav S. Sokolov,² J.-P. Rino,¹ and Nelson Studart¹

¹*Departamento de Física, Universidade Federal de São Carlos,
13565-905 São Carlos SP, Brazil*

²*B. I. Verkin Institute for Low Temperature Physics and Engineering,
National Academy of Sciences of Ukraine, 61103 Kharkov, Ukraine*

(Dated: September 10, 2018)

The mobility of surface electrons localized over helium films underlying solid substrates has been evaluated by solving the Boltzmann equation in the time relaxation approximation and the force balance equation in which an effective mobility is obtained in terms of the dynamical structure factor of the nondegenerate electron liquid. The essential processes of electron scattering by gas atoms, ripplons, and film-solid interface roughness are taken into account. The electron mobility dependence on the film thickness and temperature is determined and compared with experimental data available. We find that the interface-roughness scattering is the dominant process for explaining the experimental results. We estimate the extended defect sizes of the underlying substrate within the Gaussian correlated model for interface roughness.

PACS numbers: 73.20.-5, 7323.-b, 68.90.+g

I. INTRODUCTION

Surface electrons (SE) levitating over liquid helium has been used as a paradigmatic quasi-two dimensional electron system (Q2DES). It constitutes the counterpart of the electron system on semiconductor heterostructures in the sense that the electrons on helium obey the classical statistics because the low densities achievable in experiments ($\lesssim 10^9 \text{ cm}^{-2}$). One point difference between them comes from the scattering mechanisms. In the former system, electrons are scattered by surface excitations, the ripplons, and by vapor atoms of the helium surface. In the latter one, scattering by impurities, phonons, and interface roughness are the processes that limit the electron mobility. Besides the remarkable phenomena discovered in this low-dimensional electron system, for instance, Wigner crystallization¹ and the existence of edgemagnetoplasmons^{2,3} SE have been used as a probe to investigate the elementary surface excitations of cryogenic liquids and solids. Very recently there is an intensive search for experimental realization of SE as qubits leading to a quantum computer.^{4,5,6} For an overview of the field see Ref. 7.

For electrons trapped on the bulk helium surface it is well known that the SE mobility is dominated by the electron-helium gas atom scattering for $T > 1 \text{ K}$ whereas the SE scattering by quantized capillary waves (riplons) is responsible for mobility at lower temperatures where the helium vapor density becomes negligible. The experimental data for SE mobility over bulk helium are in reasonable agreement with theoretical calculations.⁸

The situation changes when SE are floating over a helium film which in turn is deposited over a solid substrate. In such a condition it is possible to increase significantly the accessible range of electron densities⁹ and the electron correlations may become important. Furthermore, the electron energy spectrum, the ripplon dispersion relation and the electron-riplon interaction are modified sig-

nificantly due to film effects and the van der Waals forces from the substrate now play a decisive role in the transport properties. Furthermore, besides the usual scattering mechanisms pointed out above, we must consider the SE scattering by interface defects at the helium film - substrate boundary, which, as it have been shown in experiments is responsible by the unusual behavior of the SE transport properties on a helium film.^{10,11,12,13,14}

The present work intends to provide a detailed theoretical study of the mobility of SE localized over a helium film deposited on substrates, as solid neon, glass and poly(methyl-methacrylate) [pmma], which are the materials that have been used in the experiments. We employ the Boltzmann transport equation approach (BEA) and the force balance equation method (FBEM) in which Coulomb effects on the mobility are taken into account through the dynamical structural factor of the Q2DES. We calculate the SE mobility as a function of temperature and the film thickness in the range $100 < d < 1000 \text{ \AA}$. From the comparison with experimental results we check the role of all scattering processes involved and verify the reliability of the interface roughness model used in our treatment. We find that the SE mobility is strongly determined by the interface roughness substrate and the results are in quite good agreement with the experiments.

II. BASIC RELATIONS

A. Surface electron states

Electron states on a liquid helium film are confined in the direction normal to the surface (z) due to the potential well created by a infinitely high barrier which prevents the electrons penetrate inside the liquid phase and by an attractive potential due to the electron interaction with the polarizable substrates and an applied holding electric field E_{\perp} along the z direction. The electron po-

tential energy over flat helium film located at $-d < z < 0$ is well known and given by¹⁵

$$U(z) = -\frac{\Lambda_0}{z} - \frac{\Lambda_1}{z+d} + eE_{\perp} \quad (1)$$

where $\Lambda_0 = e^2(\varepsilon_{He} - 1)/4(\varepsilon_{He} + 1)$ and $\Lambda_1 = e^2\varepsilon_{He}(\varepsilon_s - \varepsilon_{He})/(\varepsilon_{He} + 1)^2(\varepsilon_s + \varepsilon_{He})$ with ε_{He} and ε_s being the dielectric constants of helium and solid substrate, respectively, and e the electron charge.

For electrons moving freely along the helium surface with the wave function and the energy spectrum given respectively by $\psi_l(\mathbf{r}, z) = A^{-1/2} \exp(i\mathbf{k} \cdot \mathbf{r})\chi_l(z)$ and $E_l(k) = \hbar^2 k^2/2m + \Delta_l$, where \mathbf{k} and \mathbf{r} are the wave vector and position vector in the plane (x, y) of the liquid interface and A is surface area occupied by electrons. Unfortunately an analytical solution of Schrödinger equation for $\chi_l(z)$ and subbands energies Δ_l cannot be found for $U(z)$ given by Eq. (1). In this work, we use the variational method by choosing the trial wave function $\chi_1(z) = 2\gamma^{3/2}ze^{-\gamma z}$. The parameter γ depends strongly on d and is determined from the subband energy minimization as was done in Refs. 16 and 17. One has found that the energy gap between the ground and first excited subbands increases considerably by decreasing d . For example $\Delta_2 - \Delta_1 \simeq 12.7$ K for $d = 10^{-6}$ cm for the neon substrate and is much larger for a substrate with higher ε_s .¹⁷ Then one can disregard the possibility of electron transition to excited subbands which is proportional to $\exp[-(\Delta_2 - \Delta_1)/T]$ and take only the ground subband into account in the calculation of the scattering matrix elements.

B. Interaction Hamiltonians

The electron interaction with helium vapor atoms by a contact type Hamiltonian is given by

$$\hat{H}_{eg} = \frac{2\pi\hbar^2 a_0}{m} \sum_{\varepsilon, a} \delta(\mathbf{R}_e - \mathbf{R}_a) \quad (2)$$

where \mathbf{R}_e and \mathbf{R}_a are three-dimensional positions of electrons and atoms, respectively and $a_0 \simeq 0.61$ Å is the scattering length.¹⁸ The electron-ripplon interaction was derived in Ref. 15 and the electron interaction with surface roughness was obtained in the case of SE over solid hydrogen.¹⁹

Very recently two of us have constructed an Hamiltonian where both electron-ripplon and electron-solid interface interactions are treated on the same footing.²⁰ The resulting total interaction potential for any substrate was obtained from the solution of the Poisson's equation through the perturbation of the boundary conditions from the flat positions at $z = 0$ and $z = -d$. Due to very small polarizability of liquid helium, the result of our approach for the electron-ripplon interaction coincides with that obtained in Ref. 15. Bearing this in

mind, we write the Hamiltonian for the electron-ripplon and electron-interface couplings in a unique form as

$$\hat{H}_{er(ei)} = \frac{1}{\sqrt{A}} \sum_{\mathbf{q}} \xi_{1(2)\mathbf{q}} V_{r(i)\mathbf{q}}(z) e^{i\mathbf{q} \cdot \mathbf{r}}, \quad (3)$$

with¹⁵

$$V_{r\mathbf{q}}(z) = \frac{\Lambda_0 q}{z} \left[\frac{1}{qz} - K_1(qz) \right] + \frac{\Lambda_1}{(z+d)^2} + eE_{\perp}$$

and²⁰

$$V_{i\mathbf{q}}(z) = -\Lambda_1 \left\{ \left(\frac{2\varepsilon_{He}}{\varepsilon_s + \varepsilon_{He}} \right) \frac{qK_1[q(z+d)]}{(z+d)} + \left(\frac{\varepsilon_s - \varepsilon_{He}}{\varepsilon_s + \varepsilon_{He}} \right) \frac{q^2 K_2[q(z+d)]}{2} \right\},$$

where $K_j(x)$ is the modified Bessel function. Here we used the Fourier transform $\xi_j(\mathbf{r}) = A^{-1/2} \sum_{\mathbf{q}} \xi_{j\mathbf{q}} e^{i\mathbf{q} \cdot \mathbf{r}}$ for $\xi_1(\mathbf{r})$ and $\xi_2(\mathbf{r})$ and, quantizing the oscillations of free helium surface, one obtains

$$\xi_{1\mathbf{q}} = \sqrt{\frac{\hbar q \tanh(qd)}{2\rho\omega_q}} (a_{\mathbf{q}} + a_{-\mathbf{q}}^{\dagger}) \quad (4)$$

with $a_{\mathbf{q}}$ and $a_{\mathbf{q}}^{\dagger}$ being the annihilation and creation operators for ripples with wave number \mathbf{q} and satisfying the dispersion law

$$\omega_q^2 = \left(\frac{\alpha}{\rho} q^3 + g'q \right) \tanh qd, \quad (5)$$

where α is the surface tension coefficient and ρ is the density of helium. In Eq. (5), $g' = g + 3\beta/\rho d^4$, with g being the gravity acceleration and β the van der Waals constant.

Even though one cannot find from first principles the interface roughness displacement $\xi_2(\mathbf{r})$, we will use a reasonable model to calculate the interface scattering contribution to SE transport properties.

III. TRANSPORT PROPERTIES

A. Boltzmann kinetic approach

In order to calculate SE mobility along the helium surface in the presence of a driving electric field \mathbf{E}_{\parallel} we apply the well-known kinetic formalism where the electron scattering plays a crucial role in transport properties and does contribute to collision integrals in the Boltzmann equation as follows

$$\frac{e\mathbf{E}_{\parallel}}{\hbar} \frac{\partial f}{\partial \mathbf{k}} = \hat{S}_{eg} \{f\} + \hat{S}_{er} \{f\} + \hat{S}_{ei} \{f\}, \quad (6)$$

where $f(\mathbf{k})$ is the electron distribution function and $\hat{S}_{eg} \{f\}$, $\hat{S}_{er} \{f\}$, and $\hat{S}_{ei} \{f\}$ are collision integrals of

electron with helium atoms, riplons and roughness interface between the film and the substrate, respectively. By considering quasielastic scattering processes the solution of Eq. (7) is $f(\mathbf{k}) \simeq f^{(0)}(k) + f^{(1)}(k) \cos \varphi$ where $f^{(0)}(k)$ is equilibrium distribution given by the Boltzmann function for the nondegenerate Q2DES, φ is the angle between \mathbf{k} and \mathbf{E}_{\parallel} , and

$$f^{(1)}(k) = -\frac{e\mathbf{E}_{\parallel}}{\hbar\nu(k)} \frac{\partial f^{(0)}(k)}{\partial \mathbf{k}},$$

where the collision frequency $\nu(k) = \nu_{eg}(k) + \nu_{er}(k) + \nu_{ei}(k)$ and

$$\nu_j(k) = \sum_{\mathbf{k}'} W_j(\mathbf{k}', \mathbf{k}) \left(\frac{1 - f_0(k')}{1 - f_0(k)} \right) \left[1 - \frac{\mathbf{k}' \cdot \mathbf{k}}{k^2} \right]. \quad (7)$$

The probability amplitude per unit-time $W_j(\mathbf{k}, \mathbf{k}')$ for electron transition from states \mathbf{k} to \mathbf{k}' is given by Fermi's golden rule and the subscript j corresponds to each scattering mechanism whose interaction potential is given by Eqs. (2) and (3). The SE mobility is then given by

$$\mu = \frac{e}{m} \int_0^{\infty} \frac{x e^{-x} dx}{\nu(k_T x^{1/2})} \quad (8)$$

where $x = k^2/k_T^2$, with the thermal wave vector $k_T = \sqrt{2mT}/\hbar$.

The frequency of electron-atom collisions has been calculated in Ref. 18 and the result is

$$\nu_{eg} = \frac{3\pi^2 a_0^2 \hbar n_g \gamma}{8m}. \quad (9)$$

Note that ν_{eg} does not depend on k being a function of volume concentration of helium atoms $n_g = (MT/2\pi\hbar^2)^{3/2} \exp(-Q/T)$, where Q is the vaporization energy and M is the ^4He mass. As n_g is an increasingly exponential function of T , ν_{eg} becomes negligible in comparison with ν_{er} and ν_{ed} for $T < 1$ K.

The calculation of ν_{er} and ν_{ei} is more complicated. Using Eqs. (3) and (7) one can obtain in a straightforward way that both $\nu_{er}(k)$ and $\nu_{ei}(k)$ can be written as

$$\nu_{er(i)}(k) = \frac{m}{\pi\hbar^3 k^2} \int_0^{2k} \frac{q^2 \langle |\xi_{1(2)\mathbf{q}}|^2 \rangle |\langle \chi_1 | V_{r(i)\mathbf{q}}(z) | \chi_1 \rangle|^2}{\sqrt{4k^2 - q^2}} dq, \quad (10)$$

where $\langle \dots \rangle$ means an average over ensemble. Considering the electron-riplon scattering one obtains, from Eq. (4),

$$\langle |\xi_{1(2)\mathbf{q}}|^2 \rangle = \frac{\hbar q \tanh(qd)}{2\rho\omega_q} (2N_q + 1) \quad (11)$$

where the riplon number N_q is given by the Bose-Einstein function, which leads to $2N_q + 1 =$

$\coth(\hbar\omega_q/2T) \simeq 2T/\hbar\omega_q \gg 1$ for long wavelength riplons with $\hbar\omega_q \ll T$. Equation (10) results into

$$\nu_{er}(k_T x^{1/2}) = \nu_{er}^{(0)} J(x) \quad (12)$$

where $\nu_{er}^{(0)} = 8\gamma_0^2 T^2 / \pi\hbar\alpha$ and

$$J(x) = x^2 \int_0^{\pi/2} \Phi_{er}^2 \left(\sqrt{\frac{xT}{\Delta}} \sin \theta \right) \frac{\sin^6 \theta d\theta}{(\sin^2 \theta + x_c/x)} + \frac{2}{3} x \sqrt{\frac{\Delta_{\perp}^3}{\Delta_0 T^2}} \int_0^{\pi/2} \Phi_{er} \left(\sqrt{\frac{xT}{\Delta}} \sin \theta \right) \frac{\sin^4 \theta d\theta}{(\sin^2 \theta + x_c/x)} + \frac{\pi}{18} \frac{\Delta_{\perp}^3}{\Delta_0 T^2} \left[1 - \frac{x_c/x}{\sqrt{1 + (x_c/x)^2}} \right]. \quad (13)$$

Here

$$\Phi_{er}(y) = \phi(y) + \frac{\Lambda_1}{\Lambda_0 y^2} [1 + 2\gamma d + 4\gamma d(1 + \gamma d) e^{2\gamma d} Ei(-2\gamma d)], \quad (14)$$

with

$$\phi(y) = -\frac{1}{1-y^2} - \left[\frac{1}{\sqrt{(1-y^2)^3}} \ln \left(\frac{y}{1 + \sqrt{1-y^2}} \right) \right] \Theta(1-y) - \left[\frac{1}{\sqrt{(y^2-1)^3}} \arcsin \left(\frac{\sqrt{y^2-1}}{y} \right) \right] \Theta(y-1),$$

In the above expressions $\Delta = \hbar^2 \gamma^2 / 2m$, $\Delta_{\perp} = \hbar^2 \gamma_{\perp}^2 / 2m$, $\Delta_0 = m\Lambda_0^2 / 2\hbar^2$, $\gamma_{\perp} = (3meE_{\perp} / 2\hbar^2)^{1/3}$, $x_c = \hbar^2 \rho g' / 8m\alpha T$, $Ei(y)$ is the exponential-integral function, and $\Theta(y)$ is the step function.

For the scattering by interface roughness, one obtains

$$\nu_{ei}(k) = \frac{16m\Lambda_1^2 k^4}{\pi\hbar^3} \int_0^{\pi/2} \sin^6 \theta \langle |\xi_{2\mathbf{q}}(q = 2k \sin \theta)|^2 \rangle \times \Phi_{ei}^2 \left(\frac{k}{\gamma} \sin \theta \right) d\theta, \quad (15)$$

where

$$\Phi_{ei}(y) = \frac{1}{y} \int_0^{\infty} \frac{x^2 K_1 [y(x + 2\gamma d)]}{x + 2\gamma d} \exp(-x) dx. \quad (16)$$

In Eq. (16) and thereafter $K_j(x)$ is the modified j -order Bessel function. Now we must to choose an interface roughness model to derive the amplitudes $\xi_{2\mathbf{q}}$ appearing in Eq. (10). Following Prange and Nee²¹, we use the

Gaussian correlated model, in which the interface roughness is described by two characteristic sizes, the height ξ_0 and the lateral length l . These parameters define the autocorrelation function for interface roughness which can be written as

$$\langle \xi(\mathbf{r}) \xi(\mathbf{r}') \rangle = \xi_0^2 \exp\left(-\frac{|\mathbf{r} - \mathbf{r}'|^2}{l^2}\right) \quad (17)$$

which leads to

$$\langle |\xi_{2q}|^2 \rangle = \pi \xi_0^2 l^2 \exp\left(-\frac{q^2 l^2}{4}\right). \quad (18)$$

Assuming this model, the collision frequency, given by Eq. (15), can be calculated and the result is

$$\nu_{ei}(k_T x^{1/2}) = \nu_{ei}^{(0)} x F(k_T x^{1/2} l), \quad (19)$$

where $\nu_{ei}^{(0)} = 32m^2 \Lambda_1^2 \xi_0^2 T / \hbar^5$ and

$$F(b) = b^2 \int_0^{\pi/2} \sin^6 \theta \Phi_{ei}^2 \left(\frac{b}{\gamma l} \sin \theta\right) \exp(-b^2 \sin^2 \theta) d\theta. \quad (20)$$

The Gaussian correlated model was employed due to the successful description of the interface roughness for similar systems, for its simplicity and, since there are only two fitting parameters l and ξ_0 .

B. Many-electron effects

Monarkha and co-workers^{22,23,24,25} have studied electron correlation effects in the transport as well quantum magnetotransport of SE on helium by using the force balance transport equation method (FBEM). In this approach the frictional force experienced by the center of mass of the Q2DES due to electron-scatterer interactions is evaluated through the calculation of the momentum rate absorbed by the scatterers. For the system of N_e electrons the kinetic frictional force \mathbf{F}_{fr} is given by

$$\mathbf{F}_{fr} = N_e e \mathbf{E}_{\parallel} = -\frac{d\mathbf{P}}{dt}, \quad (21)$$

where

$$\frac{d\mathbf{P}}{dt} = -\frac{2\pi}{\hbar A} \left\langle \sum_{\nu', j'} (\mathbf{p}_{\nu'} - \mathbf{p}_{\nu}) |\langle \nu', j' | \hat{H}_{int} | \nu, j \rangle|^2 \delta[(E_{\nu'} + E_{j'}) - (E_{\nu} + E_j)] \right\rangle. \quad (22)$$

Here \mathbf{p}_{ν} and E_{ν} are momentum and energy of scatterer system in the state $|\nu\rangle$, E_j the energy of the electron system in the state $|j\rangle$, \hat{H}_{int} is the Hamiltonian of the interaction between the electron and the particular scatterer. The angle brackets means a thermodynamic average in the laboratory coordinate system. In Ref. 22

is was shown that $d\mathbf{P}/dt$ can be written in terms of the dynamic form factor of the Q2DES

$$S_{lab}(\mathbf{q}, \omega) = \frac{2\pi\hbar}{N_e} \left\langle \sum_{j'} |\langle j' | n_{-\mathbf{q}} | j \rangle|^2 \delta(E_{j'} - E_j - \hbar\omega) \right\rangle$$

in the laboratory frame. $S_{lab}(\mathbf{q}, \omega)$ is connected with the form factor $S(\mathbf{q}, \omega)$ in the center-of-mass of the electron system, moving at a velocity \mathbf{u} relative to the laboratory frame, as $S_{lab}(\mathbf{q}, \omega) = S(q, \omega - \mathbf{q} \cdot \mathbf{u})$. Here $n_{\mathbf{q}} = \sum_i \exp(-i\mathbf{q} \cdot \mathbf{r}_i)$. It is important to point out that electron correlations are considered in the system through the many-particle dynamic structure factor which is related to the density-density response function $\chi(q, \omega)$ through the fluctuation-dissipation theorem $S(q, \omega) = -(\hbar/2\pi n_s) \coth(\hbar\omega/2T) \text{Im}[\chi(q, \omega)]$, where n_s is the electron density.²⁶

In the limit of low velocities \mathbf{u} satisfying the condition $\hbar\mathbf{q} \cdot \mathbf{u} \ll T$, we may define an effective collision frequency as a proportionality factor between the momentum loss per unit time of the electron system and the average electron velocity as

$$\frac{d\mathbf{P}}{dt} = -m N_e \tilde{\nu} \mathbf{u}. \quad (23)$$

The effective collision frequency is the sum of frequencies for a particular interaction Hamiltonian $\tilde{\nu} = \tilde{\nu}^{(eg)} + \tilde{\nu}^{(er)} + \tilde{\nu}^{(ei)}$. The electron mobility is given then by

$$\tilde{\mu} = \frac{e}{m\tilde{\nu}}. \quad (24)$$

Substituting the interaction Hamiltonians, given by Eqs. (2) and (3), into Eq. (22) one obtains

$$\tilde{\nu}^{(eg)} = \frac{3\pi\hbar^4 \gamma a_0^2 n_g}{8m^3 T} \int_0^{\infty} q^3 S(q, 0) dq; \quad (25)$$

$$\tilde{\nu}^{(er)} = \frac{1}{4\pi m T} \int_0^{\infty} q^3 \left[\frac{\hbar q \tanh(qd)}{2\rho\omega_q} \right] \times |\langle \chi_1 | V_{rq}(z) | \chi_1 \rangle|^2 N_q S(q, \omega_q) dq. \quad (26)$$

The calculation of $\tilde{\nu}^{(ei)}$ is done in a similar way to that of $\tilde{\nu}^{(eg)}$ and the result is straightforward

$$\tilde{\nu}^{(ei)} = \frac{1}{4\pi m T} \int_0^{\infty} q^3 |\xi_{2q}|^2 \times |\langle \chi_1 | V_{iq}(z) | \chi_1 \rangle|^2 S(q, 0) dq. \quad (27)$$

In the BEFM approach, the form factor $S(q, \omega)$ is essential to the evaluation of $\tilde{\mu}$. Unfortunately $S(q, \omega)$ can be calculated analytically only in the case of the noninteracting electron system and there are no reliable approximate expressions for $S(q, \omega)$ in the whole frequency range in contrast to the static structure factor $S(k) \neq S(k, 0)$ which can be evaluated by appropriate approximation methods. In our calculations, we replace

$S(q, \omega)$ in Eqs. (25-27) by the noninteracting dynamical structure factor^{27,28}

$$S(q, \omega) = \left(\frac{2\pi m}{Tq^2} \right)^{1/2} \exp \left(-\frac{\hbar^2 q^2}{8mT} - \frac{m\omega^2}{2Tq^2} + \frac{\hbar\omega}{2T} \right) \quad (28)$$

and consider the limit $\hbar\omega_q/T \ll 1$.

IV. RESULTS AND DISCUSSION

Now we present the results of numerical calculations for SE mobility over a helium film from Eqs. (8) and (24). We have used the parameters ξ_0 and l of the electron-interface scattering to have the best fit to the mobility experimental data. First we must say that the mobility curves in the BEA and FBEM exhibit the same overall behavior independently of the adjustable parameters for the electron-interface interaction. Results for the mobility dependence on the film thickness in the BEA are presented in Fig. 1 for a glass substrate ($\varepsilon_s = 7.3$) for $T = 1.5$ K and the fitting parameters $\xi_0 = 10$ Å and $l = 1420$ Å. For a sake of comparison, we plot the mobility data taken from Ref. 13. One can see the decisive role of electron-interface scattering and the best fit is attainable for $d \lesssim 300$ Å, where, as expected, the influence of roughness is more pronounced. We also show separately the contributions to the mobility coming from electron-rippion and electron-atom scattering processes. We observe that neither electron-gas nor electron-rippion scattering mechanisms can explain the experimental data for wide range of d . By fitting the experimental data with mobility calculations in the FBEM, we obtain the best results for $\xi_0 = 6.45$ Å and $l = 5000$ Å.

In Fig. 2 we depict, in a similar way to Fig. 1, mobility curves as a function of the film thickness for solid neon ($\varepsilon_s = 1.19$) and $T = 1.2$ K. The best fit of experimental data¹⁰ is achieved for $\xi_0 = 180$ Å and $l = 300$ Å in BEA and $\xi_0 = 85$ Å and $l = 300$ Å in FBEM. We see now that ξ_0 and l are of the same order of magnitude of d which makes unjustifiable the approximation $|\zeta_2(\mathbf{r})|/d \ll 1$ which supports the perturbative approach to obtain the potential $V_{iq}(z)$ of Eq. (3), and, hence, the applicability of Born approximation for the description of electron-interface scattering. We would guess that the neon surface, being much rougher than the glass one, it has more irregularities leading to significant fluctuations of d . Moreover, we observe a worse agreement between the theoretical curve and experimental data at large d , where the electron-rippion and electron-gas mechanisms would dominated the scattering.

The temperature dependence of SE mobility is depicted in Fig. 3 where the same values for ξ_0 and l obtained by fitting $\mu(d)$ are used. As it can be seen we get rather good agreement with the experimental data of Ref. 12 for $d = 350$ Å. However the agreement becomes less satisfactory for smaller d . By considering only the electron-rippion and electron-atom scattering we found a

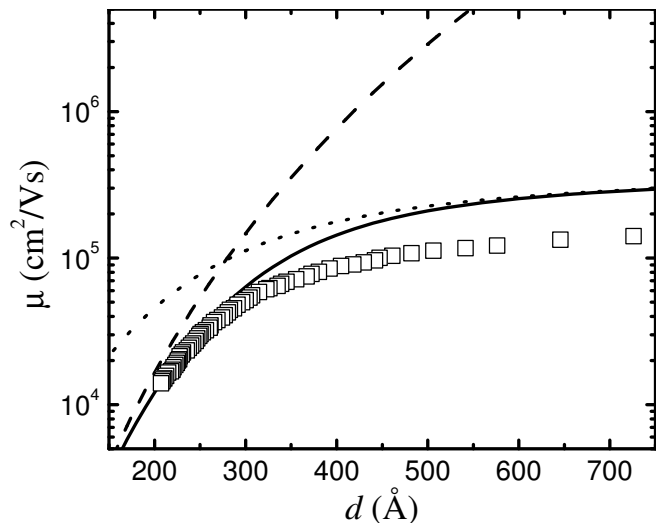


FIG. 1: Surface electron mobility as a function of the film thickness for the helium film over a glass calculated within the BEA. The solid line represents the general result when all scattering processes are taken into account. The dashed line is the contribution from interface roughness scattering and the dotted line is the sum from contributions of the electron-rippion and electron-gas scattering. The squares are experimental points of Ref. 13.

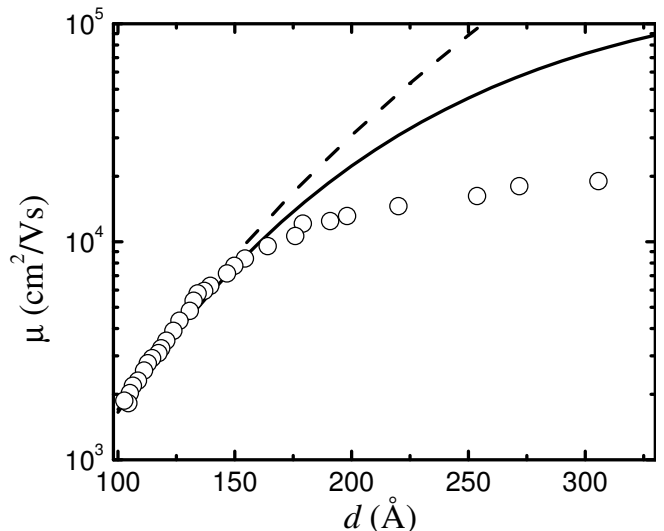


FIG. 2: Same as in Fig. 1 but for a solid neon substrate. The solid line is the contribution coming from all scattering processes and dashed line represents the mobility when only the electron-interface roughness scattering is considered. The experimental points are taken from Ref. 10.

difference of about more than one order of magnitude between the calculation results and the experimental ones. Unfortunately, to our knowledge, there is no experimental data on the temperature dependence of SE mobility in the case of a film over solid neon.

Figure 4 shows the influence of the dielectric constant

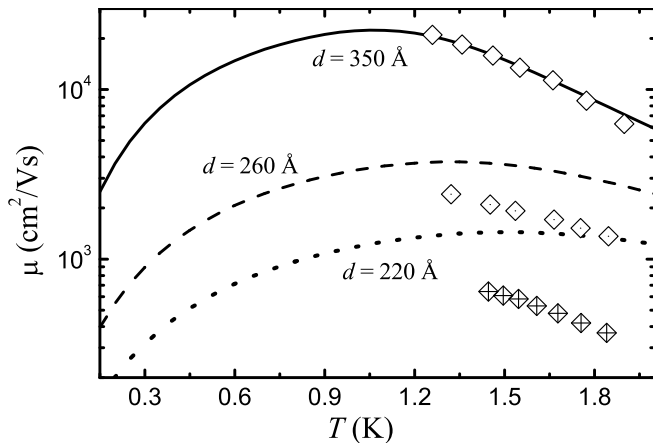


FIG. 3: SE mobility as a function of temperature including all scattering processes over a glass substrate for some values of the film thickness. The marks correspond to experimental data taken from Ref. 12.

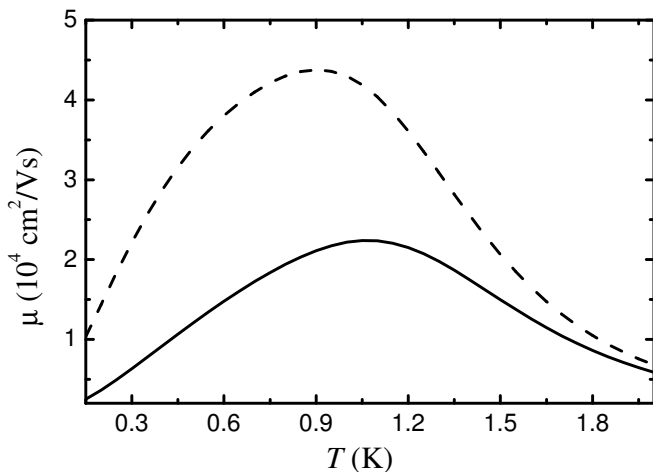


FIG. 4: Mobility versus temperature for a glass (solid line) and pmma (dashed line) substrates.

of the substrate on the SE mobility calculated within the BEA. We used here the same values of ξ_0 and l as in Fig. 1 for both glass and pmma ($\epsilon_s = 2.2$) substrates. We see that the mobility varies inversely with respect to ϵ_s for whole of temperatures considered. This is a direct consequence from $\Lambda_1 \sim \epsilon_s$ appearing in the collision frequencies which in turn are in the denominator of the mobility formulas [Eqs. (8) and (24)].

In order to make clearer the role of different scattering mechanisms we present in Fig. 5 the SE mobility, calculated within the FBEM, as a function of temperature for a film over glass and $d = 350 \text{ \AA}$. The calculated mobility curves are shown when the distinct scattering processes are considered separately. As it can be seen, the inclusion of roughness interface scattering is essential to explain the experimental data. The nonmonotonic dependence of SE mobility must be attributed to the cru-

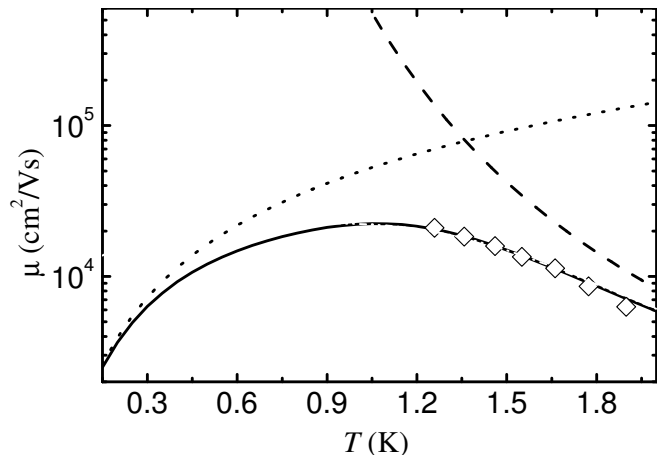


FIG. 5: Mobility as a function of the temperature calculated within the FBEM for $d = 350 \text{ \AA}$ and glass substrate. The solid line is the contribution from all scattering mechanisms whereas the dashed line is the contribution of gas scattering and the dotted line is the result for only the interface roughness scattering process.

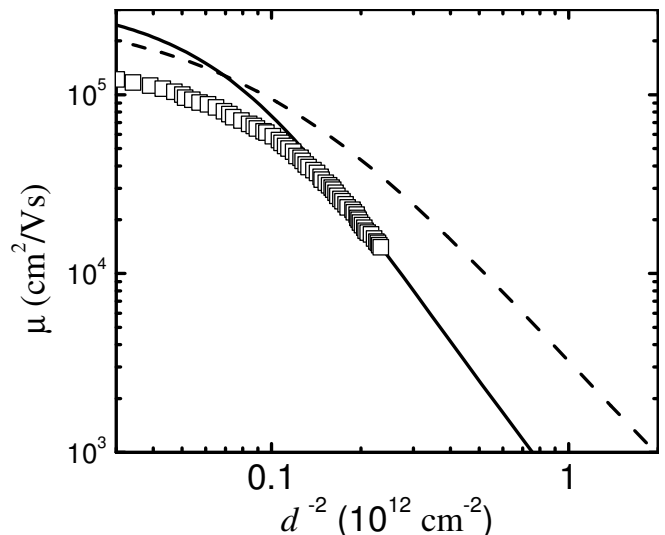


FIG. 6: Mobility as a function of the film thickness within the FBEM (solid line) and BEA (dashed line) for a glass substrate.

cial role of electron-interface scattering since it is well known that the mobility limited only by electron-rippion and electron-gas scattering is a monotonous decreasing function of temperature.

Finally, we compare the mobility results obtained in the two different methods used here by depicting the curves of $\mu(d)$ and $\mu(T)$ in Figs. 6 and 7 respectively for the case of a glass substrate. We plot also with the experimental data. Smaller values of ξ_0 obtained in FBEM as compared with those in BEA fulfill more satisfactorily the condition $|\xi_2(\mathbf{r})|/d \ll 1$. We observe much better agreement between experimental data and theo-

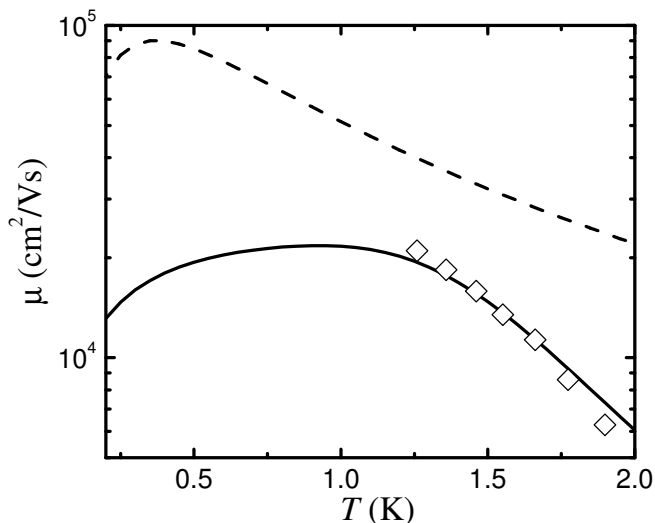


FIG. 7: Mobility as a function of temperature. The notations are the same as in Fig. 6.

retical curves calculated in FBEM for the same values of ξ_0 and l . We point out that the numerical results within the FBEM are the same as those obtained in the complete control approximation (CCA).^{29,30} In the CCA, the mobility is calculated with the BEA, but in the regime where the electron-electron collision frequency is much higher than the collision frequency due to other mechanisms. The electrons are supposed to redistribute their momenta, due to collisions between electrons, in such a way that the momentum of the total system does not change but electrons acquire the same drift velocity. The coincidence of results indicates that in order to establish the specific role of electron-electron interactions we must

go beyond the noninteracting dynamical structure factor for calculating the mobility in the FBEM as given by Eq. (28). Our conclusions then are valid only in the low or intermediate electron density regime.

V. CONCLUDING REMARKS

In this work we have studied the dependence of the mobility of surface electrons over a liquid helium film on the temperature and on the film thickness. The transport properties are determined from the solution of the Boltzmann equation in the relaxation time approximation and in the force balance equation. We employed the Gaussian correlated model to describe the interface roughness between the film and the substrate. The parameters are adjustable through the evaluation of both temperature and film thickness dependencies of the mobility. The values obtained for the strength and range of the rough interface are of the order of few atomic layers and 100 Å respectively which are reliable and in the mesoscopic regime. We showed that the SE mobility is limited by the roughness scattering because electron-rippion and electron-gas atom scattering cannot explain the experimental data. However, we cannot rule out the presence of other mechanisms as SE localization by potential wells caused by the underlying solid substrate.³¹

VI. ACKNOWLEDGMENT

We are indebted to Professor A. J. Dahm, whom forthwith provides us values of specific constants. This work was supported by CNPq and FAPESP, Brazil.

-
- ¹ C.C. Grimes and G. Adams, Phys. Rev. Lett. **42**, 795 (1979).
 - ² D.B. Mast, A.J. Dahm and A.L. Fetter, Phys. Rev. Lett. **54**, 1706 (1984).
 - ³ D.C. Glattli, E.Y. Andrei, G. Devile, J. Poitrenaud and F.I.B. Williams, Phys. Rev. Lett. **54**, 1710 (1984).
 - ⁴ A.J. Dahm, J.A. Heilman, I. Karakurt, T.J. Peshek, Physica E **18**, 169 (2003).
 - ⁵ H. Mukuda and K. Kono, RIKEN Rev. **45**, 22 (2002).
 - ⁶ G. Papageorgiou, P. Glasson, K. Harrabi, V. Antonov, E. Collin, P. Fosooni, P.G. Frayne, M.J. Lea, and D.G. Rees, and Y. Mukharsky, Appl. Phys. Lett. **86**, 153106 (2005).
 - ⁷ *Two-Dimensional Electron Systems on Helium and Others Cryogenic Substrates*, edited by E.Y. Andrei, Kluwer Acad. Publ., Dordrecht, The Netherlands (1997).
 - ⁸ Y. Iye, J. Low Temp. Phys. **40**, 441 (1980) and references therein.
 - ⁹ G. Mistura, T. Günzler, S. Nesper, and P. Leiderer, Phys. Rev. B **56**, 8360 (1997).
 - ¹⁰ P.M. Platzman, Surf. Sci. **170**, 55 (1986), reported by Dahm in Ref. 7 (see Fig. 8.1).
 - ¹¹ H.W. Jiang and A.J. Dahm, Japn. J. Appl. Phys. **26**, 745 (1987).
 - ¹² H.W. Jiang, M.A. Stan, and A.J. Dahm, Surf. Sci. **196**, 1 (1988).
 - ¹³ X.L. Hu, Y. Carmi, and A.J. Dahm, J. Low Temp. Phys. **89**, 625 (1992).
 - ¹⁴ A. J. Dahm in Ref. 7, p. 281.
 - ¹⁵ V.B. Shikin and Yu.P. Monarkha, J. Low Temp. Phys. **15**, 193 (1974).
 - ¹⁶ S.S. Sokolov, J.-P. Rino, and N. Studart, Phys. Rev. B **55**, 14473 (1997).
 - ¹⁷ S.S. Sokolov and N. Studart, Phys. Rev. B **68**, 195403 (2003).
 - ¹⁸ M. Saitoh, J. Phys. Soc. Japan **42**, 201 (1977).
 - ¹⁹ S.S. Sokolov, J.-P. Rino, and N. Studart, Phys. Rev. B **51**, 11068 (1995).
 - ²⁰ S.S. Sokolov and N. Studart, Phys. Rev. B **67**, 132510 (2003).
 - ²¹ R.E. Prange and T.W. Nee, Phys. Rev. **168**, 779 (1978).
 - ²² Yu.M. Vil'k and Yu.P. Monarkha, Fiz. Nizk. Temp. **15**, 235 (1989) [Sov. J. Low Temp. Phys. **15**, 131 (1989)].

- ²³ Yu.P. Monarkha, Fiz. Nizk. Temp. **19**, 737 (1993) [Low Temp. Phys. **19**, 530 (1993)].
- ²⁴ P.J.M. Peters, P. Scheuzger, M.J. Lea, Yu.P. Monarkha, P.K.H. Sommerfeld and R.W. van der Heijden, Phys. Rev. B **50**, 11570 (1994).
- ²⁵ Yu.P. Monarkha, E. Teske, and P. Wyder, Phys. Rep. **370**, 1 (2002).
- ²⁶ D. Pines and P. Nozières, *Theory of Quantum Liquids* (Addison-Wesley, Massachusetts, 1989).
- ²⁷ N. Studart and O. Hipólito, Phys. Rev. A **22**, 2860 (1980).
- ²⁸ H. Totsuji, Phys. Rev. B **22**, 187 (1980).
- ²⁹ D. Coimbra, S.S. Sokolov, J.P. Rino, and N. Studart, J. Low Temp. Phys. **126**, 505 (2002).
- ³⁰ S.S. Sokolov, N. Studart and D. Coimbra J. Low Temp. Phys. **138**, 409 (2005).
- ³¹ V.B. Shikin, J. Klier, I. Doicescu, A. Würfl, and P. Leiderer, Phys. Rev. B **64**, 073401 (2001).